ISSN 2070-2051, Protection of Metals and Physical Chemistry of Surfaces, 2016, Vol. 52, No. 2, pp. 211–217. © Pleiades Publishing, Ltd., 2016.
Original Russian Text © L.E. Tsygankova, V.I. Vigdorovich, A.A. Zvereva, V.I. Kichigin, 2016, published in Fizikokhimiya Poverkhnosti i Zashchita Materialov, 2016, Vol. 52, No. 2, pp. 142–149.

PHYSICOCHEMICAL PROCESSES AT THE INTERFACES

A Study of Hydrogen Accumulation in Multiwall Carbon Nanotubes by Electrochemical Techniques

L. E. Tsygankova[a], V. I. Vigdorovich[b], A. A. Zvereva[a], and V. I. Kichigin[c]

[a] *Derzhavin Tambov State University, ul. Internatsional'naya 33, Tambov, 392000 Russia*
[b] *All-Russian Scientific-Research Institute of Technics and Oil Products Usage in Agriculture, per. Novo-Rubezhnyi 28, Tambov, 392022 Russia*
[c] *Perm State University, Bukireva ul. 15, Perm, 614990 Russia*
e-mail: kichigin@psu.ru, vits21@mail.ru

Received January 13, 2015

Abstract—Accumulation of electrolytic hydrogen in alkaline medium (5 M KOH) by multiwall carbon nanotubes (MWCNTs) 20–60 nm in inner diameter and 2 μm in length obtained by catalytic pyrolysis of propane/butane mixture has been studied by means of the electrochemical diffusion technique, cyclic voltammetry, and impedance spectroscopy. MWCNTs were applied on a steel membrane and were encapsulated by a 10-nm electrolytic nickel layer. Cyclic voltammograms were recorded in the range of potentials from −1.2 to +0.2 V and contained a current peak in the cathode region corresponding to hydrogen absorption by nanotubes at −0.9 V and current peak in the anode region corresponding to oxidation of absorbed hydrogen at −0.6 V. Hydrogen storage capacity of MWCNTs varies from 4.6 to 6.5% depending on the amount of nanotubes according to electrochemical diffusion data. The electrochemical impedance data correlate with the results of the above methods.

DOI: 10.1134/S2070205116020301

INTRODUCTION

Hydrogen is a unique, highly efficient, and environmentally friendly energy source. Its usage will allow solving a number of technogenic pollution problems by means of zero-emission buildings fitted with motors running on hydrogen fuel cells. There is, however, a very serious problem in the development of hydrogen energy, namely, accumulation and transportation of hydrogen. The hydride, liquid, high-pressure or compression, and sorption at low temperatures methods proposed today do not meet the existing requirements, which will only become stricter. Hydrogen storage onboard vehicles is a problem that has not been solved to date and is a goal in many applied and basic investigations.

Thus, effective systems are those that contain at least 6.5 wt % of hydrogen or no less than 63 kg m^{-3} according to regulations of the US Department of Energy, whereas the standards of the International Energy Agency dictate at least 5 wt % of hydrogen in carrier extracted from a battery at $T \leqslant 373$ K. Developing devices that meet these specified requirements is necessary to realize the possibilities of hydrogen energy progress, as well as solving problems of raw materials and energy on Earth and, in general, sustainable development of the world's population.

After carbon nanotubes were discovered in 1991 [1], their ability to store hydrogen attracted wide attention. The carbon nanostructured materials considered as hydrogen storages, unsurprisingly, receive increasing attention because the methods to produce them are widely developed. There are two types of such materials that differ in ability to accumulate hydrogen, namely, carbon nanotubes (CNTs) and carbon nanofibers (CNFs), on the one hand, and fullerenes, on the other. The difference between them is in the nature of binding, i.e., the location of hydrogen in a battery.

At the same time, it is a common feature of the carbon materials that their surface has oxide compounds, typically quinone, phenolic, lactone, and carboxyl groups, and much less frequently hydroperoxide, anhydrite, and heterocyclic ones [2–6]. In addition, the surfaces of diverse technical carbon [2–6] and fibrous carbon materials [7–10], carbon nanotubes [11], and carbon composites [12–14], as well as pyrolytic graphite [15], also contain these functional groups. The nature of such compounds is qualitatively almost independent of state and material of substrate [16], whereas functional groups are reduced at sufficient cathodic polarization. In such a case, a hydrogen evolution reaction that corresponds to the laws of electrochemical kinetics proceeds on surfaces that have been purified from oxide chemicals. However, when

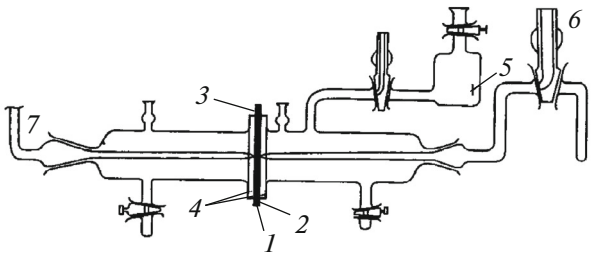

Fig. 1. Scheme of Devanathan cell: (*1*) membrane, (*2*) contact with input or polarization side of membrane, (*3*) contact with output or diffusion side of membrane, (*4*) washer (fluoroplastic), (*5*) auxiliary electrode (smooth Pt), and (*6*) and (*7*) electrolytic key.

no cathodic polarization is used, the oxide compounds form rapidly again on the surface, implying that oxygen and hydrogen are obtained from the carbon phase. This observation, in particular, is supported by the fact that electroconductivity of carbon materials changes throughout the sample thickness [8–10].

CNTs have seamless graphene sheet as an essential element. Multiwall CNTs (MWCNTs) exist as a coiled graphene sheet.

There are two experimental ways to pump CNTs by hydrogen. One of them is the high-pressure method, which leads to physical sorption of hydrogen molecules [17, 18] between tufts in the intratube space [19–21]. The maximum hydrogen storage capacity ranges from 3 to 6% in such conditions [19, 21]. It is desirable, however, to store hydrogen gas at room temperature and at a pressure less than 10 atm. A serious disadvantage of this method is that experiments are reproduced poorly because of strong dependence on sample preparation conditions [22].

Another method of hydrogen storage is to pump MWCNTs electrochemically [23–26]. It has been proposed that hydrogen is adsorbed on carbon nanotubes as ions throughout the electrochemical process. The hydrogen storage capacity, however, is no more than 1 wt % [23]. The very small capacitance values for SWCNTs and MWCNTs vary from 0.2 to 3.7 wt % according to some studies [23, 27–30]. These values are probably due to experimental errors, a high content of microporous or amorphous carbon in samples, or the use of additives to increase conductivity of electrodes. When using high-purity SWCNTs and MWCNTs, hydrogen storage capacity does not exceed 0.2–0.4 wt % [31, 32].

In some cases, carbon nanotubes are believed to be unable to store large amounts of hydrogen, and when storage takes place this amount is insignificant [23, 27–30]. In addition, there are published results of current–voltage measurements in which anode current peaks are due to metal impurities that used as catalysts to prepare carbon nanotubes, but are not due to hydrogen oxidation. The high values of hydrogen storage were also determined incorrectly in some works [33, 34].

The accumulation and distribution of hydrogen in composite SWCNTs encapsulated by thin palladium layers on a palladium substrate upon electrolytic hydrogenation have been studied [35]. Using vacuum thermal desorption and voltammograms, these authors have shown that SWCNTs increase capacity of Pd/SWCNT composite material relative to hydrogen up to 24–26% upon electrolytic hydrogenation compared to pure palladium. The SWCNT capacity in composite material depends on volume ratio between Pd and SWCNTs and comprises 12% at V(Pd)/V(SWCNT)>10.

The aim of this work is to study adsorption of electrolytic hydrogen by MWCNTs.

EXPERIMENTAL

MWCNTs were obtained by catalytic pyrolysis of propane/butane mixture (70 vol % of C_3H_8) at 625 ± 25°C with Ni/Mg catalyst having 80- to 500-μm dispersity applied on a substrate of 100- to 400-μm thickness. The inner diameter of MWCNTs comprised 20–60 nm, the length was 2 μm, and the specific surface area was 144 $m^2\ g^{-1}$ [36]. The MWCNTs were produced by OOO NanoTechCentre in Tambov, Russia.

MWCNTs obtained directly after synthesis were treated with diluted HNO_3 solution to dissolve the remaining catalyst. These nanotubes then were boiled for 2 h at 106 ± 2°C in a mixture of concentrated HNO_3 and H_2SO_4 to remove catalyst residues and amorphous carbon. The crystallinity of MWCNTs has been confirmed by X-ray data.

The absorption of electrolytic hydrogen by carbon nanotubes was studied with the use of the electrochemical diffusion technique, voltammetry, and electrochemical impedance spectroscopy.

The electrochemical diffusion technique entails the use of Devanathan cells [37] (Fig. 1) with a vertical steel membrane having 300-μm thickness and 3.63-cm^2 area, on which a certain amount of water–ethanol solution of MWCNTs modified with polyvinylpyrrolidone was applied. After a liquid phase has evaporated, electrolytic sedimentation of nickel with 10-nm thickness from a standard nickel plating electrolyte containing $NiSO_4$, Na_2SO_4, NaCl, and H_3BO_3 was performed to encapsulate MWCNTs. The membrane prepared by this approach was placed then in a Devanathan cell. The cathode polarized side of this membrane, together with MWCNTs, was in contact with 5 M KOH stock electrolyte solution, whereas the diffusion one was in contact with titrated $KMnO_4$ solution. The atomic hydrogen adsorbed on membrane surface and produced by the reaction

$$H_2O + e \rightarrow H_{ads} + OH^-$$

forms partially hydrogen molecules and is then moved into the gas phase, is partially absorbed by nanotubes, and is partially diffused through the membrane into $KMnO_4$ solution, wherein it is oxidized. A similar experiment was carried out without MWCNTs using a steel membrane on which an electrolytic nickel layer of the same thickness was applied as in those experiments with MWCNTs. The difference in the amount of hydrogen oxidized with potassium permanganate in the absence and presence of MWCNTs on the membrane is consistent with its absorption by nanotubes.

The rate of hydrogen mass transfer (i_H, A m^{-2}) through a steel membrane positioned vertically and modified with MWCNTs was determined at room temperature using the Kardash–Batrakov approach [38]. The duration of an individual experiment was 2 h. The front side of membrane was polarized potentiostatically at $E = -1.2$ V in an IPC-Pro potentiostat. The potentials were measured relative to a saturated silver chloride electrode and recalculated to the normal hydrogen scale. Average strength of polarizing current ($I_к$) at a given potential was calculated using quantity of electricity Q defined from chronoamperogram (I–τ) by integration. The calculations were performed with the same strength of polarizing cathode current in absence and in presence of MWCNTs.

Current of hydrogen diffusion I_H was calculated according to the formula

$$I_H = \frac{mF}{E\tau},$$

where m is weight of hydrogen diffused through membrane, F is the Faraday constant, E is equivalent weight of hydrogen, and τ is time.

The I_H value corresponding to the amount of hydrogen absorbed by tubes is calculated by the difference of hydrogen diffusion current in the absence and presence of MWCNTs on the membrane. Using the I_H value, weight of hydrogen m_H accumulated by MWCNTs and the storage capacity of hydrogen were calculated as follows:

$$\eta_H = (m_H/m_{MWCNTs}) \times 100\%.$$

The quantity of hydrogen absorbed by MWCNTs was also determined by another method.

After a cathode side of a membrane came into contact with the MWCNTs/Ni composite in 5 M KOH solution at $E = -1.2$ V for 2 h to saturate electrode by hydrogen, the potential was switched from −1.2 to −0.6 V at which hydrogen oxidation occurred in the same solution. The current peak in a chronoamperogram (CA) has indicated this process. The potential of hydrogen oxidation was determined preliminarily using voltammograms. Quantity of electricity Q that was used to oxidize hydrogen was determined by integration of CA current peak of hydrogen oxidation. The same experiment was carried out without MWCNTs using a membrane coated with the same nickel weight as in the Ni/MWCNTs system.

The electricity quantity (Q_{MWCNTs}) corresponding to oxidation of hydrogen absorbed by MWCNTs was determined with the formula $Q_{MWCNTs} = Q_{MWCNTs + Ni} - Q_{Ni}$, where $Q_{MWCNTs + Ni}$ is the total amount of electricity that was used to oxidize hydrogen in MWCNTs/Ni composite and Q_{Ni} is amount of electricity which was utilized to oxidize hydrogen absorbed by nickel. The content of hydrogen per unit weight of MWCNTs was calculated by the formula $\eta_H = QE/(Fm_{MWCNTs})$.

Voltammograms were recorded in the range from −1.2 to +0.2 V in forward and backward directions at a 0.66-mV/s scanning speed.

The electrochemical impedance of electrodes was studied in the frequency range ($\omega/2\pi$) from 10 kHz to 50 MHz with an ac voltage amplitude of 10 mV using electrochemical measurement equipment produced by Solartron Co. (United Kingdom) including an SI 1255 impedance analyzer and SI 1287 potentiostat. A steel membrane with a 3.63-cm^2 working area with a certain amount of MWCNTs coated with a 10-nm nickel layer served as the working electrode. The membrane and the auxiliary platinum electrode were placed into a Devanathan double-chamber cell. The polarization part of the cell was filled only by working solution, while the diffusion part was filled by 0.01 N $KMnO_4$ solution. The saturated aqueous silver chloride electrode was used as a reference one. All the potentials were converted into a normal hydrogen scale.

Electrochemical impedance data processing was carried out with ZView 3.0 software, which enables performing calculations using any equivalent schemes with up to 20 elements on the basis of changes in complex impedance of an electrochemical system with a frequency including real and imaginary parts of a complex number. The initial values of all the elements of an equivalent scheme chosen randomly were specified preliminarily. To avoid finding a function local minimum, a calculation was repeated many times with different initial values of scheme elements. Root mean square deviation s was the evaluation criterion of schemes; the equivalent scheme was satisfactory at $s \leqslant 5\%$.

RESULTS AND DISCUSSION

Figure 2 shows SEM images of a steel membrane surface with applied MWCNTs: (a) without encapsulation by nickel layer and (b) with it.

The amount of hydrogen absorbed by MWCNTs in alkaline solutions at $E = -1.2$ V to be calculated using data of six parallel experiments indicated that the specific capacity of hydrogen storage (η_H %) decreases

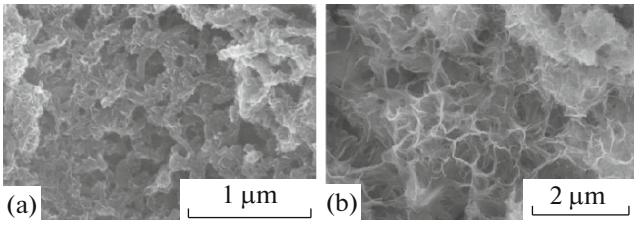

Fig. 2. SEM images of a steel membrane surface with applied MWCNTs: (a) without encapsulating by nickel layer and (b) with it.

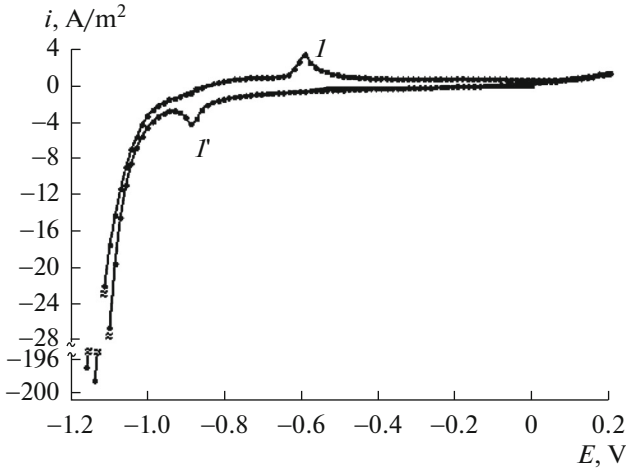

Fig. 3. Voltammograms of a steel membrane with 96 μg of MWCNTs encapsulated by electrolytic nickel layer in 5.0 M KOH: (1) forward direction; (1') reverse one.

slightly with increasing weight of MWCNTs applied on the membrane (Table 1). This, however, requires checking by other approaches. Similar results were obtained previously when experiments were performed using 1M KOH solution with a membrane and MWCNTs encapsulated by electrolytic iron [39].

Figure 3 shows voltammograms. The current peak in the cathode region at $E = -0.9$ V corresponds to saturation of an electrode coated by MWCNTs/Ni composite by hydrogen. The peak ascribed to oxidation of absorbed hydrogen was observed using reverse scanning potential at $E = -0.6$ V. No peaks were registered when no MWCNTs were on the electrode.

Table 2 provides experimental results on switching the polarization of membrane with MWCNT layer

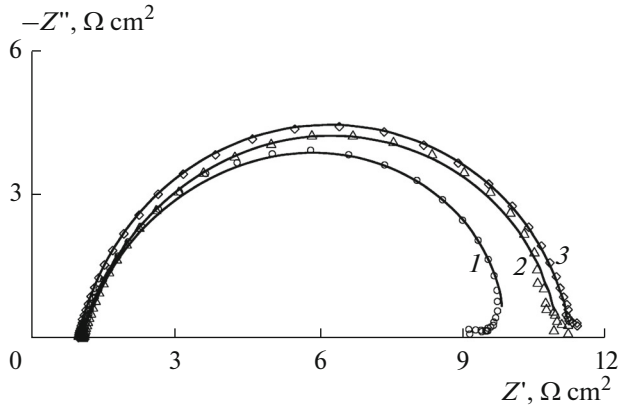

Fig. 4. Nyquist diagrams of membrane coated with MWCNTs (96 μg) and encapsulated by nickel electrolytic layer with 10-nm thickness at $E = -1.2$ V in 5 M alkali solution. The points correspond to experimental data; the lines correspond to fitting in accordance with equivalent scheme. The numbers of curves denote cycle number.

encapsulated by nickel (96 μg) from cathode potential at −1.2 V after 2-h exposure to hydrogen oxidation potential at −0.6 V and subsequent determination of electricity quantity corresponding to oxidation of absorbed hydrogen.

The hydrogen content per weight unit of MWCNTs was determined using an average value of Q calculated on the basis of data from Table 2 and an amount of electricity in an idle test without MWCNTs on membrane and was found to be 4.7%, so that it is in satisfactory agreement with the data of Table 1.

Impedance hodographs were measured with membrane having MWCNTs applied on the entire surface in an amount of 96 μg and encapsulated by an electrolytic nickel layer in 5 M KOH solution at $E = -1.2$ V (Fig. 4): immediately upon application of the potential (first cycle), after exposure at a given potential for half an hour (second cycle), and then 1 h (third cycle). The same measurements were carried out with a nickel-plated membrane without MWCNTs (Fig. 5). The impedance graphs on a complex plane are close to semicircles. Either some systematic deviations from the semicircle because of incomplete stationary system (first cycle in Figs. 4 and 5) or a random scatter of points due to effect of generated hydrogen (second and third cycles) were observed at the lowest frequencies.

Only that frequency range in which there were no significant deviations of this type was used for processing.

Table 1. Hydrogen absorption by MWCNTs in 5.0 M KOH at $E = -1.2$ V and upon encapsulation by a 10-nm nickel layer

m_{MWCNTs} on membrane, mg	No MWCNTs	0.032	0.048	0.096
I_H, A	2.04×10^{-4}	2.02×10^{-5}	3.04×10^{-5}	1.09×10^{-5}
η_H, %	–	6.5	4.8	4.6

With respect to the measurement results in Devanathan cell, impedance spectra processing was carried out in accordance with the equivalent scheme (Fig. 6) that corresponds to the molecular hydrogen evolution reaction (MHER) in the presence of hydrogen absorption [40–42]. When selecting an equivalent scheme, the fact that hydrogen absorption by iron in alkaline solutions occurs throughout the adsorbed state [43] was taken into consideration. The equivalent scheme (Fig. 6) involves elements of Faraday impedance in MHER, R_1, R_2, and C_2 (their physical meaning was discussed elsewhere [41, 44]), resistance to absorption reaction, i.e., transition steps of H_{ads} into the subsurface position (R_{abs}), as well as diffusion impedance of hydrogen atoms in the membrane (Z_d). The diffusion impedance is generally expressed by the formula

$$Z_d = R_d \frac{\text{th}(j\omega\tau_d)^{p_d}}{(j\omega\tau_d)^{p_d}},$$

where R_d is diffusion resistance and τ_d represents characteristic diffusion time ($\tau_d = d^2/D$, in which d is membrane thickness and D is diffusion coefficient). A fixed value $p_d = 0.5$ was used.

Calculation of the hydrogen diffusion coefficient D in steel membrane, using characteristic time τ_d = 10.0–11.5 s without MWCNTs on the membrane (Table 3) and excluding the effect of the 10-nm nickel layer on hydrogen permeability of membrane, gives $D = (7.8–9.0) \times 10^{-5}$ cm^2/s, which is in good agreement with that of published data obtained for iron from 7.8×10^{-5} to 8.3×10^{-5} cm^2/s at 22–25°C [45–47].

The hydrogen permeability of membranes measurements indicate that some amount of hydrogen is retained by nanotubes, i.e., MWCNTs can be hydrogen traps. The impedance of hydrogen absorption based on hydrogen-capturing traps or impedance of ion implantation into materials containing trap invading particles were discussed in [42, 48, 49]. It has been obtained [48] an expression of hydrogen diffusion impedance with its capture by traps using the McNabb and Foster model [50] which postulates that capture probability is proportional to the concentration of diffusing hydrogen atoms and to concentration of vacant traps. An equal distribution of traps throughout membrane cross section was considered in [48], and accepted boundary conditions corresponded to impermeable border in membrane output side. It was concluded [48] that the impedance plot of pure diffusion and diffusion of hydrogen with its capture by traps has the same pattern for both reversible and irreversible capture. The same result would probably be obtained for the permeate boundary. Hydrogen capture by MWCNTs can lead to an increase in characteristic diffusion time because traps can decrease effective hydrogen diffusion coefficient in the solid state. The data from Tables 3 and 4 indicate that the ratios $\tau_{d,\,\text{MWCNTs}}/\tau_{d,\,0}$ ($\tau_{d,\,\text{MWCNTs}}$ and $\tau_{d,\,0}$ are diffusion time values in absence and in presence of MWCNTs, respectively) comprise 1.04, 1.22, and 1.30 in first, second, and third cycles, respectively; in other words, impedance data probably indicate that there is hydrogen capture by carbon nanotubes applied on an electrode membrane surface.

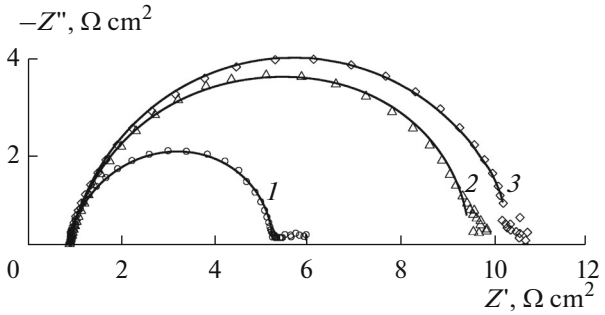

Fig. 5. Nyquist diagrams of membrane encapsulated by nickel layer with 10-nm thickness without MWCNTs at $E = -1.2$ V in 5 M alkali solution. The points correspond to experimental data and lines correspond to fitting according to equivalent scheme. The numbers of curves denote cycle number.

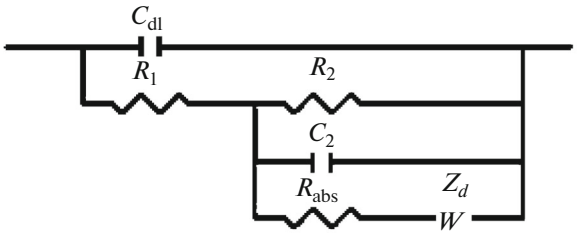

Fig. 6. The equivalent scheme for MHER and hydrogen absorption reaction.

The findings obtained from impedance measurements should be taken with some caution despite satisfactory accuracy in describing experimental impedance spectra using an equivalent scheme (Fig. 6) and relatively small errors in determining parameters of equivalent scheme (Tables 3 and 4). This is due to the following factors: (1) the hydrogen absorption reaction has a small contribution to immittance of the electrode, so that there is a small difference between Nyquist plots and right semicircles; this factor complicates the distinct impedance process models, wherein

Table 2. Amount of electricity used to oxidize hydrogen absorbed by MWCNTs (96 μg)/Ni composite at $E = -0.6$ V in 5 M KOH solution

№	1	2	3	4	5	6
Q, C	0.5847	0.2353	0.5591	0.6221	0.5119	0.3746

Table 3. Numerical values of equivalent scheme elements for a steel membrane coated with a 10-nm nickel layer upon $E = -1.2$ V in 5 M KOH solution

	1st cycle	2nd cycle	3rd cycle
C_{dl}, μF/cm^2	469 (1.3)*	380 (2.7)	287 (4.5)
R_1, Ω cm^2	2.6 (6.9)	1.8 (4.9)	2.4 (11.1)
R_2, Ω cm^2	1.9 (6.1)	7.6 (2.7)	7.6 (0.8)
C_2, μF/cm^2	954 (39.3)	227 (6.2)	189 (2.7)
R_{abs}, Ω cm^2	19.3 (3.9)	24.3 (14.4)	24.7 (21.5)
R_d, Ω cm^2	78.0 (3.5)	78.4 (19.2)	58.8 (9.5)
τ_d, s	11.5 (7.8)	10.0 (7.2)	10.6 (12.5)
p_d	0.5	0.5	0.5
χ^2/sum	0.000425/0.0302	0.000420/0.0265	0.000205/0.0129

* The numbers in brackets are parameter error in %; sum is sum of square deviations.

Table 4. Numerical values of equivalent scheme elements for steel membrane coated by MWCNTs (96 μg) and encapsulated by a 10-nm nickel layer upon $E = -1.2$ V in 5 M KOH solution

	1st cycle	2nd cycle	3rd cycle
C_{dl}, μF/cm^2	392 (1.8)*	518 (3.1)	387 (2.4)
R_1, Ω cm^2	3.1 (3.7)	3.4 (29.5)	1.4 (17.5)
R_2, Ω cm^2	7.2 (1.5)	10.8 (4.6)	9.5 (26.4)
C_2, μF/cm^2	562 (3.4)	784 (1.9)	290 (4.5)
R_{abs}, Ω cm^2	29.2 (15.9)	14.6 (7.8)	11.1 (4.2)
R_d, Ω cm^2	30.5 (13.2)	2.2 (12.4)	2.2 (9.7)
τ_d, s	12.0 (13.4)	12.1 (2.5)	13.9 (13.2)
p_d	0.5	0.5	0.5
χ^2/sum	0.000331/0.0228	0.000531/0.0419	0.000348/0.0229

* The numbers in brackets are parameter error in %; sum is sum of square deviations.

there is a stage of hydrogen penetration into the solid phase, and obtaining reliable values of hydrogen absorption impedance parameters for a particular model; (2) scattered points at the lowest frequencies that somewhat reduces the accuracy in determining impedance parameter values of hydrogen absorption reaction. It can be supposed, however, that there is a qualitative agreement between results of hydrogen permeability of membrane measurements and impedance spectroscopy.

CONCLUSIONS

The accumulation of electrolytic hydrogen by multiwall carbon nanotubes encapsulated with a thin electrolytic nickel layer in 5 M KOH solution has been studied. The storage capacity of electrolytic hydrogen in MWCNTs ranges from 4.6 to 6.5% according to the electrochemical diffusion technique data. The findings obtained with the use of electrochemical impedance spectroscopy are in qualitative agreement with the data.

REFERENCES

1. Iijima, S., *Nature,* 1991, vol. 354, p. 56.
2. Fialkov, A.S., *Formirovanie struktury i svoistva uglegrafitovykh materialov* (Structuring and Properties of Coal-Graphite Materials), Moscow: Metallurgiya, 1965.
3. Fialkov, A.S., *Uglegrafitovye materialy* (Coal-Graphite Materials), Moscow: Energiya, 1979.
4. Pechkovskaya, K.A., *Sazha kak usilitel' kauchuka* (The Implementation of Soot for Reinforcement of Caoutchouc), Moscow: Khimiya, 1968.
5. Tarasevich, Yu.G., *Elektrokhimiya uglerodnykh materialov* (Electrochemistry of Carbo Materials), Moscow: Nauka, 1984.
6. Shvartsman, A.S. and Fialkov, A.S., *Zh. Prikl. Khim.,* 1987, vol. 60, p. 1559.
7. Varentsov, V.K. and Varentsova, V.I., *Khim. Interesakh Ustoich. Razvit.,* 2000, vol. 8, no. 3, p. 353.
8. Varentsov, V.K. and Varentsova, V.I., *Russ. J. Appl. Chem.,* 2000, vol. 73, no. 10, p. 1742.
9. Varenstov, V.K. and Varentsova, V.I., *Russ. J. Electrochem.,* 2001, vol. 37, no. 7, p. 690.

10. Varenstov, V.K., Varentsova, V.I., Bataev I.A. Yusin S.I., *Prot. Met. Phys. Chem. Surf.,* 2011, vol. 47, no. 1, p. 43.
11. Shibaev, D.A., Orlov, V.Yu., Bazlov, D.A., and Vaganov, V.Yu., *Khim. Khim. Tekhnol.*, 2011, vol. 54, no. 7, p. 38.
12. Vigdorovich, V.I., Tsygankova, L.E., Aleksashina, E.V., and Gladysheva, I.E., Korroz.: Mater., Zashch., 2010, no. 1, p. 8.
13. Vigdorovich, V.I., Tsygankova, L.E., Kichigin, V.I., and Gladysheva, I.E., *Prot. Met. Phys. Chem. Surf.,* 2012, vol. 48, p. 207.
14. Vigdorovich. V.I., Tsygankova, L.E., Kichigin, V.I., and Gladysheva, I.E., *Prot. Met. Phys. Chem. Surf.,* 2012, vol. 48, p. 438.
15. Tsygankova, L.E., Aleksashina, E.V., Gladysheva, I.E., and Vigdorovich, V.I., *Kondens. Sredy Mezhfaznye Granitsy,* 2009, vol. 11, no. 3, p. 249.
16. Bannov, A.G., Varentsov, V.K., Chukanov, I.S., Gorodilova, E.V., and Kuvshinov, G.G., *Prot. Met. Phys. Chem. Surf.,* 2012, vol. 48, no. 2, p. 199.
17. Pan, W., Zhang, X., Li, S., et al., *Int. J. Hydrogen Energy,* 2005, vol. 30, p. 719.
18. Zhou, L., Zhou, Y., and Sun, Y., *Int. J. Hydrogen Energy,* 2006, vol. 31, p. 259.
19. Dillon, A.C., Jones, K.M., Bekkedahl, T.A., et al., *Nature*, 1997, vol. 386, p. 377.
20. Ye, Y., Ahn, C.C., Witham, C., et al., *Appl. Phys. Lett.,* 1999, vol. 74, p. 2307.
21. Liu, C., Fan, Y.Y., Liu, M., et al., *Science,* 1999, vol. 286, p. 1127.
22. Darkrim, F.L., Malbrunot, P., and Tartaglia, G.P., *Int. J. Hydrogen Energy,* 2002, vol. 27, p. 193.
23. Nutzenadel, C., Zuttel, A., Chartouni, D., and Schlapbach, L., *Electrochem. Solid-State Lett.,* 1999, vol. 2, p. 30.
24. Vix-Guterl, C., Frackowiak, E., Jurewicz, K., et al., *Carbon,* 2005, vol. 43, p. 1293.
25. Zhang, H., Fu, X., Chen, Y., et al., *Physica B,* 2004, vol. 352, p. 66.
26. Chen, X., Zhang, Y., Gao, X.P., et al., *Int. J. Hydrogen Energy,* 2004, vol. 29, p. 743.
27. Qin, X., Gao, X.P., Liu, H., et al., *Electrochem. Solid-State Lett.,* 2000, vol. 3, p. 532.
28. Rajalakshmi, N., Dhathathreyan, K.S., Govindaraj, A., and Satishkumar, B.C., *Electrochim. Acta,* 2000, vol. 45, p. 4511.
29. Fazle Kibria, A.K.M., Mo, Y.H., Park, K.S., et al., *Int. J. Hydrogen Energy,* 2001, vol. 26, p. 823.
30. Gundiah, G., Govindaraj, A., Rajalakshmi, N., et al., *J. Mater. Chem.,* 2003, vol. 13, p. 209.
31. Lee, S.M., Park, K.S., Choi, Y.C., et al., *Synth. Met.,* 2000, vol. 113, p. 209.
32. Zuttel, A., Sudan, P., Mauron, P., et al., *Int. J. Hydrogen Energy,* 2002, vol. 27, p. 203.
33. Jones, C.P., Jurkschat, K., Crossley, A., et al., *Langmuir,* 2007, vol. 23, p. 9501.
34. Niessen, R.A.H., de Longe, J., and Nottena, P.H.L., *J. Electrochem. Soc.,* 2006, vol. 153, p. A1484.
35. Solodkova, L.N., Lyakhov, B.F., Lipson, A.G., and Tsivadze, A.Yu., *Prot. Met. Phys. Chem. Surf.,* 2010, vol. 46, no. 5, p. 524.
36. Tkachev, A.G., *Perspekt. Mater.,* 2007, no. 3, p. 5.
37. Devanathan, M.A.V. and Stachurski, Z., *Zashch. Met.,* 1995, vol. 31, p. 441.
38. Tsygankova, L.E., Vigdorovich, V.I., and Zvereva, A.A., *Prot. Met. Phys. Chem. Surf.,* 2013, vol. 49, p. 669.
39. Lim, C. and Pyun, S.-I., *Electrochim. Acta,* 1993, vol. 38, p. 2645.
40. Lasia, A., in *Modern Aspects of Electrochemistry,* Conway, B. and White, R., Eds., New York: Kluwer, 2002, vol. 35, p. 1.
41. Gabrielli, C., Grand, P.P., Lasia, A., and Perrot, H., *J. Electrochem. Soc.,* 2004, vol. 151, p. A1925.
42. Bockris, J.O.M., McBreen, J., and Nanis, L., *J. Electrochem. Soc.,* 1965, vol. 112, p. 1025.
43. Harrington, D.A. and Conway, B.E., *Electrochim. Acta,* 1987, vol. 32, p. 1703.
44. Dull, D.L. and Nobe Ken, *Corrosion,* 1979, vol. 35, p. 535.
45. Saito, Y. and Nobe Ken, *Corrosion,* 1980, vol. 36, p. 178.
46. Zakroczymski, T., *Scr. Mater.,* 1985, vol. 19, p. 521.
47. Diard, J.-P., *J. Electroanal. Chem.,* 2003, vol. 557, p. 19.
48. Bóbics, L., Sziráki, L., and Láng, G.G., *Electrochem. Comm.,* 2008, vol. 10, p. 283.
49. McNabb, A. and Foster, P.K., *Trans. Metall. Soc. AIME,* 1963, vol. 227, p. 618.

Translated by A. Tulyabaev